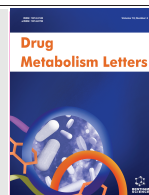


Rate-Determining and Rate-Limiting Steps in the Clearance and Excretion of a Potent and Selective p21-Activated Kinase Inhibitor: A Case Study of Rapid Hepatic Uptake and Slow Elimination in Rat



Peter W. Fan^{1,*}, Jacob Z. Chen¹, M. Allan Jaochico¹, Hank La¹, Ning Liu¹, Teresa Mulder¹, Robert T. Cass¹, Matthew Durk¹, Kirsten Messick², Nicole Valle², Shannon Liu², Wendy Lee³, James J. Crawford³, Joachim Rudolph³, Lesley J. Murray¹, S. Cyrus Khojasteh¹ and Matthew Wright¹

¹Department of Drug Metabolism and Pharmacokinetics; ²Non-Clinical Operations; ³Medicinal Chemistry, Genentech, Inc., 1 DNA Way, South San Francisco, CA 94080, USA



Peter W. Fan

Abstract: *Background:* Significant under-prediction of *in vivo* clearance in rat was observed for a potent p21-activated kinase (PAK1) inhibitor, GNE1.

Objective: Rate-determining (rapid uptake) and rate-limiting (slow excretion) steps in systemic clearance and elimination of GNE1, respectively, were evaluated to better understand the cause of the *in vitro-in vivo* (IVIV) disconnect.

Methods: A series of *in vivo*, *ex vivo*, and *in vitro* experiments were carried out: 1) the role of organic cation transporters (Oct or Slc22a) was investigated in transporter knock-out and wild-type animals with or without 1-aminobenzotriazole (ABT) pretreatment; 2) the concentration-dependent hepatic extraction ratio was determined in isolated perfused rat liver; and 3) excreta were collected from both bile duct cannulated and non-cannulated rats after intravenous injection.

Results: After intravenous dosing, the rate-determining step in clearance was found to be mediated by the active uptake transporter, Oct1. In cannulated rats, biliary and renal clearance of GNE1 accounted for only approximately 14 and 16% of the total clearance, respectively. *N*-acetylation, an important metabolic pathway, accounted for only about 10% of the total dose. In non-cannulated rats, the majority of the dose was recovered in feces as unchanged parent (up to 91%) overnight following intravenous administration.

Conclusion: Because the clearance of GNE1 is mediated through uptake transporters rather than metabolism, the extrahepatic expression of Oct1 in kidney and intestine in rat likely plays an important role in the IVIV disconnect in hepatic clearance prediction. The slow process of intestinal secretion is the rate-limiting step for *in vivo* clearance of GNE1.

Keywords: Enzyme-transporter interplay, hepatic uptake, intestinal secretion, IVIVC, Organic cation transporter.

Received: March 02, 2016

Revised: April 04, 2016

Accepted: April 05, 2016

INTRODUCTION

Because of increased demand for novel therapeutic options for difficult-to-treat diseases as well as the advancement in small molecule drug design and medicinal chemistry tools, many chemical entities do not exhibit textbook drug-like ADME properties. Lipinski's rule of five has been continuously challenged and pushed to the limit in creative drug design [1-3]. Consequently, an increased number of discovery molecules are cleared *via* permeability-limited mechanisms, representing a shift away from traditional perfusion-limited clearance mechanisms. When the clearance mechanism is perfusion-limited, the standard practice is to use well-established *in vitro* metabolic stability and traditional metabolite identification assays to predict and characterize major elimination pathways, respectively. When

clearance is limited by permeability, however, metabolic rates from *in vitro* systems are no longer a good predictor of *in vivo* clearance. Rather, the rate of influx into cells such as hepatocytes becomes the major determining factor for *in vivo* clearance [4]. Therefore, improved *in vitro-in vivo* (IVIV) correlation is expected when the rate of influx is incorporated into the prediction for this class of molecule [1]. Technologies to measure active hepatic uptake (influx) and efflux *in vitro* have made tremendous progress in the past decade [5-8]. In general, however, they are better suited for more-advanced drug candidates rather than those from early high-throughput screens because these assays are often labor intensive and cell isolation (i.e., of hepatocytes) and cryo-preservation are known to be associated with the loss of uptake transporter activity. In addition, many of the active uptake and efflux transporters are not well characterized in these models. For example, it is known that basolateral uptake transporters (OATP and OCT) and sinusoidal efflux transporters (MRP3 and MRP4) are still active in suspended hepatocytes but canalicular efflux transporters (such as Pgp,

*Address correspondence to this author at the Genentech, Inc., 1 DNA Way, MS 412a, South San Francisco, CA 94080, USA; Tel: +1 650 225-6808; E-mail: fan.peter@gene.com

MRP2, and BCRP) are internalized and, therefore, not functional [9].

One of the most studied p21-activated kinase members, PAK1, is an attractive therapeutic target for cancer as it is thought to play an important role in cell motility and cytoskeletal organization [10-13]. PAK1 is widely expressed in normal tissues and overexpressed in cancer cells such as bladder, breast, ovary and others [11, 12]. Therefore, significant drug discovery efforts have been made to find a potent inhibitor of this class [14-16]. In late stage drug discovery, a series of highly potent and selective PAK1 inhibitors, the 2,4-diaminopyrimidines, was tested for rat pharmacokinetic (PK) parameters [17]. In general, many of these compounds exhibited exceptionally high clearance in rat. They often exceeded hepatic blood flow (Table 1). *In vitro*, however, these compounds were relatively stable in rat hepatocytes and/or microsomes. Additionally, this class of molecule can undergo a significant amount of *N*-acetylation, while cytochrome P450 (P450)-mediated metabolism might play only a minor role [17]. Since *N*-acetyltransferase, NAT1, is expressed ubiquitously [18], the source of the IVIV disconnect was believed to be due to extrahepatic metabolism. The team put forth a significant effort to reduce *N*-acetylation by the use of structure activity relationships (SARs). However, despite improvements in metabolic stability in both rat liver microsomes/S9 and hepatocytes as well as a reduction in the extent of *N*-acetylation, GNE3 (Table 1) was still cleared rapidly in rat, suggesting that other clearance mechanisms were involved. Given its similarity in potency and structure to GNE3, GNE1¹ was selected for additional characterization. GNE1 was found to be an Organic Cation Transporter (OCT1) substrate in human, and Oct1 played a significant role in the clearance of this compound in rodent [1]. The compound was rapidly taken up by rat hepatocytes with hepatic uptake rate comparable to that of atorvastatin [1]. In the absence of Oct transporters (1 and 2), clearance of GNE1 was reduced by half [1]. To further confirm the rate-determining step in the clearance of this compound and understand its elimination fate in rat after an intravenous dose, we: 1) carried out additional *in vivo* studies by inhibiting oxidative metabolism and *N*-acetylation with 1-aminobenzotriazole (ABT) in both Oct1/2-double knockout (KO) and wild-type mice; 2) quantified unchanged GNE1 and its major metabolite, GNE4, in bile, urine and feces from rat; 3) performed and isolated perfused rat liver experiment. The results of these experiments suggest that GNE1 is rapidly removed from systemic circulation in plasma, slowly metabolized in liver, and slowly eliminated, mainly by intestinal excretion, in rat. Liver, possibly kidney and intestine as well, may serve as efficient reservoirs for trapping GNE1, thus preventing it from entering the systemic circulation.

MATERIALS AND METHODS

Chemicals and Reagents

GNE1, *N*²-(((1*r*,4*r*)-4-aminocyclohexyl)methyl)-5-chloro-*N*⁴-(5-cyclopropyl-1*H*-pyrazol-3-yl)pyrimidine-2,4-diamine;

GNE2, *N*²-(((1*r*,4*r*)-4-aminocyclohexyl)methyl)-*N*⁴-(5-cyclopropyl-1*H*-pyrazol-3-yl)pyrimidine-2,4-diamine; GNE3, 2-(4-aminopiperidin-1-yl)-*N*-(5-cyclopropyl-1*H*-pyrazol-3-yl)thieno[3,2-*d*]pyrimidin-4-amine; and the *N*-acetylated metabolite of GNE1 (GNE4), *N*-((1*r*,4*r*)-4-(((5-chloro-4-((5-cyclopropyl-1*H*-pyrazol-3-yl)amino)pyrimidin-2-yl)amino)methyl)cyclohexyl)acetamide were synthesized in-house (supplemental method). Acetyl coenzyme A (acetyl-CoA) sodium salt, 1-aminobenzotriazole (ABT), bovine serum albumin, ethylenediaminetetraacetic acid (EDTA), indomethacin, ketamine/xylazine HCl solution, Krebs-Henseleit buffer, labetalol, loperamide, and polyethylene glycol (PEG400) were purchased from Sigma-Aldrich (St. Louis, MO). Tetrasodium salt of NADPH was obtained from EMD Millipore (Billerica, MA). All other reagents and solvents of highest quality were purchased from commercial vendors.

Intrinsic Clearance Determination of GNE2 and GNE3 in Liver S9 in the Presence of NADPH and Acetyl-CoA; and in Hepatocytes

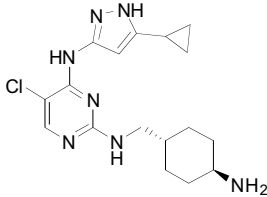
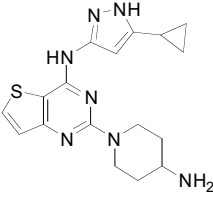
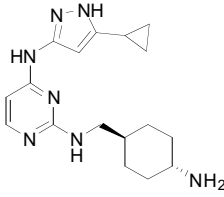
Briefly, the rates of NADPH- or acetyl-CoA- (1 mM final) dependent metabolism were assessed for GNE1, 2 and 3 (0.5 μM final) in one of the following *in vitro* systems as described in previous publications [19, 20]: liver microsomes (at 0.5 mg/mL protein), S9 (at 2 mg/mL protein) or hepatocytes (0.5 million cells/mL). Parent compound disappearance over time (calculated using the substrate depletion method) was monitored using the analytical method described previously [19, 20]). Scaling factors used for the calculation of intrinsic clearance [21] were 45 mg of protein per gram of liver (both rat and human) for microsomal incubations, 165 mg of protein per gram of liver for rat S9 incubations [22], and a liver weight of 40 and 25.7 g per kg for rat and human, respectively. For hepatocytes, incubations were carried out as described previously [21]. Scaling factors of 135 and 120 million cells per gram of liver were used for rat and human, respectively.

Metabolite Identification of GNE1 in Mouse Hepatocytes with or without ABT

Briefly, cryopreserved mouse hepatocytes from Celsis *In Vitro* Technologies (Baltimore, MD) were used and incubations at 1 million cells per mL were carried out under 5% CO₂ and 37 °C according to the manufacturer's thawing and incubation instructions. The hepatocytes were spiked with GNE1 as a DMSO stock solution to a final concentration of 5 μM and a final DMSO concentration of 0.1% in incubations with or without ABT. ABT was prepared in water, and the final ABT concentration was 500 μM. The reaction was quenched with 3 mL acetonitrile at 0 and 3 hours and centrifuged at 2000 × *g* for 5 minutes. The resulting supernatant was reduced to a dry residue and reconstituted with 300 μL water:methanol (2:1; volume to volume [v/v]) prior to LC-MS/MS analysis. Metabolite identification was carried out on an Accela (Thermo Fisher Scientific, San Jose, CA) HPLC coupled with an Orbitrap Velos (Thermo Fisher Scientific). Separation of metabolites was achieved using Acquity CSH C18 column (1.7 μm, 2.1 x 100 mm; Waters, Milford, MA) with a flow rate of 0.4 mL/min of mobile phases (A) 0.1% formic acid in water and (B) 0.1% formic

¹Preliminary *in vitro* data including OCT1 and hepatic uptake and pharmacokinetic properties of GNE1 were published previously in Future Medicinal Chemistry (2014). GNE1 is equivalent to compound 1 in the abovementioned manuscript.

Table 1. *In vitro* hepatic uptake and metabolic rates via either P450 or N-acetyltransferase and pharmacokinetic parameters for the p21-activated kinase inhibitors GNE1, GNE2, and GNE3.

	GNE1	GNE2	GNE3
			
PAK1 K_i (nM)	26	22	26
MW/Log $D_{pH=7.4}$ /tPSA	362/0.83/104	355/0.48/95	327/-0.2/104
Kinetic solubility (μ M)	157	72	136
MDCK A \rightarrow B P_{app} ($\times 10^{-6}$ cm/s)	0.1	0.4	0.5
MDCK efflux ratio	43	13.5	6.2
HLM/HH CL_{int} (mL/min/kg)	4.5/2.4	8.6/7.6	9.1/4.5
RLM/RH CL_{int} (mL/min/kg)	6.1/34	62/91	8.3/10
CL_{int} of P450 metabolism in rat S9 (mL/min/kg)	ND	<10	<10
CL_{int} of N-acetylation in rat S9 (mL/min/kg)	ND	337	21
CL_{int} hepatic uptake in rat (mL/min/kg) ¹	11.1	ND	ND
<i>In vivo</i> rat CL_p (mL/min/kg) IV bolus	216	>>hepatic blood flow	160
f_u rat	0.16	0.22	0.25
f_u perfusate	0.3	ND	ND
f_u liver homogenate (undiluted)	0.02	ND	ND

¹Value taken from previous reference [1].

A \rightarrow B P_{app} , apparent permeability in the apical to basolateral direction; CL_{int} , intrinsic clearance; f_u , the unbound fraction; HH, human hepatocytes; HLM, human liver microsomes; IV, intravenous; K_i , inhibition constant; Log $D_{pH=7.4}$, octanol/buffer partition coefficient at pH 7.4; MW, molecular weight; ND, not determined; P450, cytochrome P450; RH, rat hepatocytes; RLM, rat liver microsomes; tPSA, topological polar surface area. Scaling factors for the CL_{int} determination are described in detail under Materials and Methods.

acid in acetonitrile. HPLC gradients were initiated with 95% A for 1 minute followed by 80% A over the next 14 minutes. The column was then washed with a pulse of 95% B for 2 minutes and returned to the initial composition of 95% A for an additional 2 min. The electrospray ion source was set at 3-5 kV and the heated capillary temperature at 360°C. High resolution mass measurements were performed using external calibration. Data-dependent multistage mass spectrometry (MSⁿ) scans were acquired.

Pharmacokinetic experiment performed in female Oct1/2 double targeted mutation knockout (KO) and wild-type (FVB/N) mice in the presence or absence of ABT. All *in vivo* studies were carried out in accordance with the Guide for the Care and Use of Laboratory Animals as adopted and promulgated by the United States National Institute of Health. Transporter KO and the corresponding wild-type animals were 9 to 14 weeks of age (Taconic Farms, Hudson, NY). The study was divided into four groups with N=3 for each group: wild-type with or without ABT and Oct1/2 double KO with or without ABT. For the ABT treatment groups, animals were first dosed 100 mg/kg ABT in water at 5 mL/kg *via* oral gavage. Animals that did not receive ABT

were given an equal volume of water instead. Two hours later, all animals received a solution formulation of GNE1 in 40% PEG400 at 2 mg/kg in the tail vein, and the dosing volume was kept 5 mL/kg. Blood samples (15 μ L) were collected at serial time points at predose, 0.03, 0.25, 0.5, 1.0, 3.0 and 6.0 hours postdose *via* tail nick. An EDTA solution (4 x the blood volume) was added to each of the blood samples, which were immediately frozen and stored at -80°C pending analysis. The blood concentration of GNE1 was analyzed after thawing and protein precipitation by acetonitrile treatment. The standard curve of GNE1 was constructed in diluted blood (same dilution factor as the sample treatment, i.e., 4 x the blood volume) containing EDTA to correct for the any possible ion suppression due to EDTA.

Intravenous Bolus and Infusion of GNE1 in Sprague-Dawley Rats

Briefly, for pharmacokinetic experiments conducted in Sprague-Dawley rats purchased from Charles River (Wilmington, MA), the animals were fasted overnight and given either an intravenous bolus or infusion dose of GNE1

at 2 mg/kg dissolved in either 60% PEG or 35/10/55% PEG400/DMSO/water at pH 4 *via* femoral or jugular vein cannula, respectively. Dosing volume was capped at 2 mL/kg. For the bolus experiment, blood samples were collected *via* the jugular vein cannula, and plasma was isolated immediately in EDTA blood collection tubes. Samples were collected at predose, 0.03, 0.08, 0.25, 0.5, 1, 2, 4, 6, 8, and 24 hours. The intravenous infusion experiment was carried out in a similar manner with the same dose and volume except that GNE1 was slowly infused at 0.57 mg/kg/h at a rate of 1 mL/h/kg. Infusion was continued for 3.5 hours to achieve approximately 90% of steady state based on its terminal half-life ($t_{1/2}$) obtained from intravenous bolus dose. Plasma was collected at predose, 0.5, 2, 3.5, 3.53, 3.58, 3.75, 4.25, 5.5, 7.5, and 24 hours. In addition to plasma, urine, at 0–7.5 and 7.5–24 hours and feces, over 24 hours, were collected from the infusion experiment. Concentrations of GNE1 and its major metabolite GNE4 were determined in the plasma, urine, and fecal samples using LC/MS/MS.

Pharmacokinetic Experiment of GNE1 in Bile Duct Cannulated Rat

Bile duct cannulated (BDC) Sprague-Dawley rats were purchased from Charles River (Wilmington, MA). Upon acclimation, the animals were fasted overnight prior to intravenous bolus treatment of GNE1. They were then dosed at 2 mg/kg *via* jugular vein cannula in a vehicle consisting of 60% PEG400. The dose volume was 2 mL/kg. Bile samples were collected *via* bile duct cannula predose and in 0–4, 4–8, 8–24, 24–48, and 48–72 hours postdose intervals. Additionally, urine and feces were collected predose and at 0–8, 8–24, 24–48, and 48–72h postdose intervals. Concentrations of GNE1 and its major metabolite GNE4 were determined in the bile, urine, and fecal samples using LC/MS/MS.

Single-pass Isolated Perfused Liver from Rat

Isolated perfused liver experiment was carried as described in previous publications [23, 24]. Briefly, adult male Sprague-Dawley rats (350–400 g) were used as liver donors. The rats were anesthetized by an intraperitoneal injection of a ketamine/xylazine cocktail and, after opening the abdominal cavity, the hepatic portal vein was catheterized with a 14-gauge IV catheter to serve as an inlet. After cutting the diaphragm, another IV catheter, inserted into the thoracic inferior vena cava, served as an outlet. The liver was then excised and transferred to a temperature-controlled perfusion tray. The isolated livers were perfused using a commercial perfusion apparatus (MX Perfuser II; MX International, Aurora, CO) in a single pass manner.

The perfusate consisted of a Krebs-Henseleit bicarbonate buffer (pH 7.35–7.45) containing glucose (5.0 g/L), bovine serum albumin (4%, w/v), and bovine red blood cells (20%, v/v), delivered at a flow rate of 12 mL/min. The perfusate was oxygenated with an O₂:CO₂ (95:5) mixture for at least 30 minutes before entering the liver. In addition, the common bile duct was cannulated using PE-50 tubing. The viability of the liver was confirmed through overall macroscopic appearance of the liver, the color of the inlet and outlet perfusate, and the extent of perfusate and bile flow.

At the start of the perfusion experiment, different concentrations of GNE1 in DMSO stock (0.3–8.3 μM final concentration; less than 0.1% final concentration of organic solvent) was cassette dosed together with a known high hepatic extraction ratio marker, propranolol, in water (2–4 μM final) and added to the perfusate reservoir. In a separate set of experiment, quinine (10 μM final), a potent OCT1 inhibitor, was also included to examine the importance of uptake transporter. At 20, 40, 60, 80, and 110 minutes, an aliquot of the perfusate (200 μL) was sampled from both the inlet and outlet. At the end of the experiment, liver was saved and flash frozen in liquid nitrogen and stored at -80°C until analysis. Finally propranolol, GNE1 and its acetylated metabolite (GNE4) were quantified in bile, perfusate, and liver. The viability of the liver was confirmed through the overall macroscopic appearance of the liver, the color of the inlet and outlet perfusate, and the extent of perfusate and bile flow.

Quantitation of GNE1 and GNE4 Total Concentration and Metabolite Identification in Rat Bile, Feces, Liver, Liver Perfusate, Plasma, and Urine

All biological samples were frozen and stored at -80°C prior to analysis. Briefly, after thawing, liver or fecal samples from the experiments described above were first homogenized with 2- or 4-fold (w/v) water, respectively. Standard curves and quality control samples were prepared by spiking a known amount of a mixture of GNE1, GNE4 and propranolol (the latter from the isolated perfused liver experiment only) into blank matrices composed of one of the following: bile, fecal homogenate, liver homogenate, liver perfusate, plasma, or urine. Mixed general internal standards (labetalol, 100 ng/mL; indomethacin, 100 ng/mL; and loperamide, 10 ng/mL) in acetonitrile (200 μL) were added to 25 μL of the samples. Following vortex and centrifugation at 1500 x g for 10–15 minutes, 100 μL of supernatant was transferred to a 96-well plate and diluted with 50 μL water prior to analysis by HPLC-MS/MS. The analytical system consisted of a Shimadzu Nexera X2 UHPLC and autosampler (Shimadzu, Columbia, MD) and an AB Sciex API 6500 QTrap (AB Sciex, Foster City, CA) mass spectrometer with a turbo ion spray interface. A 20 μL aliquot of each sample was injected onto a reverse-phase Kinetex XB-C18 30 x 2.1 mm, 2.6 μm column (Phenomenex, Torrance, CA). The lower limit of quantitation (LLOQ) ranged from 0.8 to 2.0 ng/mL. The assay accuracy was between 75% and 125%. Dilution factors were incorporated for all tissue samples.

For metabolite identification in fecal and liver homogenates, and in plasma and liver perfusate, samples were treated with acetonitrile, centrifuged, dried and reconstituted as described before. For bile and urine samples, the precipitate was removed *via* centrifugation (3000 x g). They were then injected directly into the LC-MS/MS for analysis as described above.

Liver to Perfusate Total and Unbound Ratio of GNE1, K_p, and K_{p,u}, Determination

The observed partition coefficient ($K_{p, \text{observed}}$) was calculated as the total tissue concentration (liver) divided by the outflow perfusate total concentration measured at the end

of the perfusion or incubation. Aliquots of liver homogenate (previously diluted 2-fold) and perfusate from the above isolated perfused liver experiment were loaded into a 96-well rapid equilibrium dialysis chamber (Thermo Scientific, Waltham, MA) and dialyzed against phosphate buffer for 4 hours according to the manufacturer's instructions. A longer equilibration time did not increase the unbound fraction, suggesting that equilibrium was achieved after 4 hours of incubation (data not shown). To account for dilution (D) during homogenization, the unbound fraction was back-calculated according to the following equation, as described in a previous publication [25]:

$$\text{Undiluted } f_u = \frac{1/D}{\left[\left(\frac{1}{f_{u,\text{measured}}} \right)^{-1} \right]^{+1/D}} \quad (1)$$

$K_{p_{u,u}}$ was obtained by factoring the ratio of unbound tissue concentration to the unbound perfusate concentration [26].

Pharmacokinetic Analysis

Intravenous pharmacokinetic parameters were estimated using the WinNonLin software package (Pharsight, Mountain View, CA). Total blood or plasma clearance (CL_{iv}), renal clearance (CL_{urine}), biliary clearance (CL_{bile}), the apparent terminal half-life ($t_{1/2}$), and steady state volume of distribution (V_{ss}) of GNE1 were calculated based on Lau *et al.*'s method [27].

Data and Statistical Analysis

Data are expressed in the mean \pm standard deviation. One-way ANOVA and the dependent T test (GraphPad Software, Inc., San Diego, CA) were used to compare the changes in blood clearance from Oct1/2 double KO versus wild-type animals and also from ABT versus non-treated groups. A *p*-value of less than 0.05 was considered to be statistically significant.

RESULTS

N-acetylation and Oxidative Metabolism of GNE1, GNE2 and GNE3 *in vitro*

Metabolic stability of GNE2 and GNE3 was first compared systematically across liver microsomes, S9, and hepatocytes (Table 1). P450-dependent metabolism was first measured in the presence of NADPH, and then *N*-acetylation was examined separately using acetyl-CoA as the cofactor. Between these two potent PAK1 inhibitors, GNE2 was extensively *N*-acetylated in rat liver S9 with intrinsic clearance (CL_{int}) reaching 337 mL/min/kg. P450-dependent oxidative metabolism was very low in the same system. GNE3, on the other hand, was much more stable metabolically towards both oxidative metabolism and *N*-acetylation by several folds in rat S9. Despite the high rate of clearance for GNE2 in S9 with different cofactors, the compound nevertheless showed a less than 2-fold difference in CL_{int} between hepatocytes and NADPH-dependent metabolism in rat liver microsomes. Furthermore, despite the significant metabolic stability improvement of GNE3 over GNE2 in rat microsomes and hepatocytes by at least 3-fold, both of these

PAK1 inhibitors have similar (2-fold or less difference) metabolic stability in human hepatocytes and microsomes after scaling. The rate of oxidative metabolism and *N*-acetylation for GNE1 was not examined in rat S9 because this compound is significantly more stable than GNE2 in rat. This stability suggests that the thiophene ring in GNE2 is important for binding to *N*-acetyltransferase.

In Vitro Metabolite Identification of GNE1 in Mouse Hepatocytes with or without ABT

After treating mouse hepatocytes with GNE1, two metabolites were tentatively characterized (supplemental data). M1 was an oxidative metabolite (+16 Da), and M2 was identified as GNE4 (*N*-acetylated) because it had the same retention time and MS/MS fragmentation as the synthetic standard. No further effort to characterize M1 was performed as this metabolite was not detected in rodents *in vivo* (data not shown).

Effect of ABT on the Clearance of GNE1 in Oct1/2 Double KO and Wild Type Mice

After treating the animals orally with 100 mg/kg ABT, the blood clearance of GNE1 (intravenous (IV), 2 h post ABT dose) was reduced by 20.5% in the wild-type versus 28.2% in the double KO mice, corresponding to an average overall decrease of 24% (Fig. 1). This decrease is about 2.3-fold smaller than that seen between the wild-type and the transporter KO mice blood clearance regardless of ABT treatment, in which a 56% average change was observed.

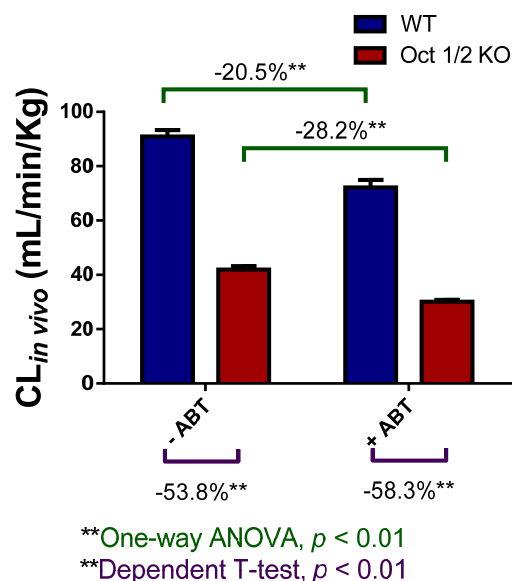


Fig. (1). Blood clearance of GNE1 (dosed *via* IV bolus) 2 hours after pretreatment of wild-type and double knock-out mice with 100 mg/kg of ABT. ABT, 1-aminobenzotriazole; $CL_{in\ vivo}$, *in vivo* clearance; KO, knock-out mice; WT, wild-type mice. Results are the average of three animals per group. One-way ANOVA and dependent T-test are described in Materials and Methods. Green lines = percentage reduction in clearance between ABT treatment group versus that without treatment in the same strain of mice. Purple lines = percentage reduction in clearance between WT and KO mice. A *p*-value of less than 0.05 was considered to be statistically significant.

These differences were all statistically significant based on One-way ANOVA and the dependent T-test.

Intravenous Bolus Versus Infusion of GNE1

When dosed in rat, GNE1, GNE2, and GNE3 all exhibited clearances that were greater than hepatic blood flow. When dosed as bolus in rat, the clearance of GNE1 reached 216 ± 53 mL/min/kg with a volume of distribution reaching 20.5 ± 1.9 L/kg (Fig. 2 and Table 2A). An infusion of GNE1 to 90% of steady state reduced clearance by half to 121 ± 4 mL/min/kg and volume by 5-fold to 4.2 ± 1.2 L/kg. Renal clearance was found to be 20 ± 1.2 mL/min/kg. The blood to plasma ratio was previously determined to be 1.2 [1].

Table 2A. Pharmacokinetic parameters of GNE1 after dosing as IV bolus and IV infusion to 90% of steady state.

Dosing Route, <i>n</i> = 3	IV Bolus, 2 mg/kg	IV Infusion, 0.57 mg/kg/h@1 mL/kg/h
Plasma CL (mL/min/kg)	216 ± 53.0	121 ± 4.35
V_{ss} (L/kg)	20.5 ± 1.92	4.21 ± 1.16
Terminal half-life (h)	1.32 ± 0.43	0.74 ± 0.10
CL _B (mL/min/kg)	21.5 ± 6.20	ND
CL _R (mL/min/kg)	49.7 ± 3.84	20.2 ± 1.22

CL, clearance; CL_B, biliary clearance; CL_R, renal clearance; IV, intravenous; ND, not determined; V_{ss} , steady state volume of distribution. Blood to plasma ratio for GNE1 was previously determined to be 1.2 [1]

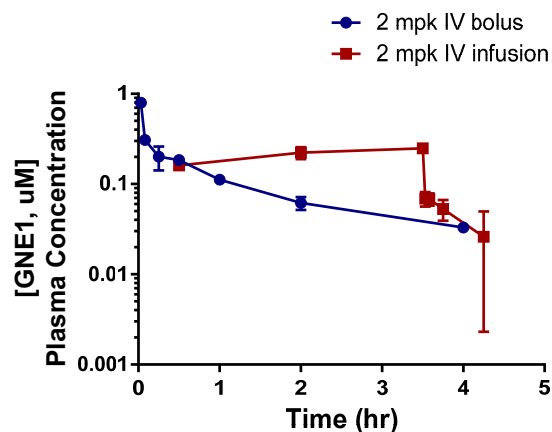


Fig. (2). Pharmacokinetics of 2 mg/kg GNE1 following IV bolus or IV infusion in rat. Infusion rate was 0.57 mg/kg/hour at 1 mL/kg/hour and continued until 3.3 half-lives (3.3 hours) or approximately 90% of steady state. Results are the average of three animals for each group.

Recovery of GNE1 in Bile, Feces, and Urine

The amount of unchanged GNE1 was further quantified in bile, feces, and urine. The amount excreted was high over 24 hours, but the overall rate of excretion was slow as most of the inhibitor was recovered during the overnight collection (Table 2B). In the absence of bile collection, the total amount of GNE1 recovered in urine over 24 hours was 16%. In BDC rats, however, a significant shift was observed in the percentage of parent recovered in urine as an approximately 2-fold increase was observed; a total of 30%

Table 2B. Collection of GNE1 in excreta up to 24 hours.

	Dose recovery of Unchanged GNE1 (% of Total Dosed)									
	Bile			^a Feces		Urine			Total Recovery	
Time points	0-4h	4-8h	8-24h	0-8h	8-24h	0-4h	4-8h	8-24h		
Intact, <i>n</i> = 3	NA			77 ± 36		8.5 ± 2.3			7.1 ± 2.0	93
^b BDC, <i>n</i> = 3	7.8 ± 1.2	2.5 ± 0.9	3.9 ± 1.8	5.8 ± 4.2	18 ± 4.7	BQL	30 ± 1.1	2.8 ± 1.0		71

^aAmount of GNE4 or *N*-acetylated metabolite of GNE1 detected in feces = $9.5 \pm 4.8\%$; a negligible amount was detected in urine.

^bBDC rats were replenished with sodium taurocholate as described in the Materials and Methods.

BDC, bile duct cannulated; BQL, below the quantifiable limit; NA, not applicable.

Table 2C. Collection of GNE1 in excreta up to 72 hours.

	Dose recovery of Unchanged GNE1 (% of Total Dosed)						
	Bile		^a Feces		Urine		Total Recovery (24-72 h)
Time points	24-48h	48-72h	24-48h	48-72h	24-48h	48-72h	
Intact, <i>n</i> = 3	NA		8.4 ± 2.9	<1	<1	<1	8.4
^b BDC, <i>n</i> = 3	<1	0	2.2 ± 1.4	<1	<1	<1	2.2

^aRecovery of GNE1 in feces during 0-24 hours was 91 ± 17 (intact) vs. 31 ± 10 (BDC); amount of GNE1 (unchanged) in bile and urine during 0-24 hours was about 15% combined. The *N*-acetylated metabolite GNE4 level remained around 10% or less (not shown).

^bBDC rats were replenished with sodium taurocholate as described in the Materials and Methods
BDC, bile duct cannulated; NA, not applicable.

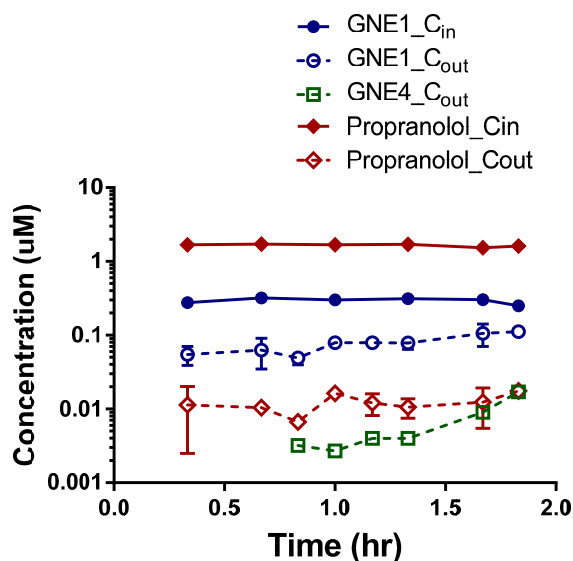


Fig. (3). Representative C_{in} (inlet) and C_{out} (outlet) of GNE1 at 0.3 μM , propranolol at 2 μM , and GNE4 in isolated perfused rat liver. Results are the average of three experiments. Single-pass perfusion was performed as described in Materials and Methods.

of GNE1 was recovered in urine at 4-8 hours post IV dose. Changes in urinary volume were not significant during the 0-4 and 4-8 hour time intervals in BDC rats (6.9 mL vs. 5.9 mL, respectively). Furthermore, no significant change in fecal weight was observed between the animal groups (data not shown). Overall biliary excretion of unchanged GNE1 was low, averaging 14%. Fecal recovery of unchanged GNE1 was high, with intact animals excreting up to 77% over 24 hours. Again, a shift in percentage of recovery in feces was observed in BDC rats as these rats excreted only 24%, approximately 3-fold less than the fecal recovery in intact animals. Because of the poor recovery observed in BDC rats, another set of experiments was performed to compare intact versus BDC rats with an excreta collection time of up to 72 hours (Table 2C). The excretion pattern was

similar to that seen before, but recovery did not improve significantly in BDC rats. Treatment of BDC rats with activated charcoal did not significantly improve parent molecule recovery (data not shown).

GNE4, the major metabolite of GNE1, was also monitored in the excreta after IV dosing. The amount detected of this *N*-acetylated metabolite was low, totaling approximately 13- and 8-fold less than the parent compound in urine, feces, and bile combined over the course of 72 hours in intact and BDC rats, respectively (supplemental data). As a result of its low recovery, GNE4 was deemed an insignificant metabolite and was not extensively studied.

Liver Perfusion, Hepatic Extraction Ratio, and $K_{p_{u,u}}$ Determination

To understand hepatic contribution to the total clearance of GNE1, an isolated perfused liver (IPL) experiment in rat was performed. Steady state was achieved *via* single-pass perfusion (Fig. 3). Both propranolol and GNE1 showed a high hepatic extraction ratio (ER; >0.95 and 0.78, respectively; Table 3). Biliary elimination was slow for GNE1 ($CL_{biliary} = 0.7 \text{ mL/min/kg}$), at about 26-fold lower than the calculated GNE1 perfusate clearance. Very little *N*-acetylated metabolite was detected, suggesting that metabolism was slow. At the end of the perfusion experiment, the total GNE1 concentrations in the liver homogenate and C_{out} were measured (8 and 0.07 μM , respectively). The intracellular to extracellular ratio of unbound concentrations ($K_{p_{u,u}}$) was then determined to be 3.8 after factoring in the corresponding free liver and perfusate fractions and total concentrations.

To further examine the effect of drug concentration to the uptake transporter, GNE1 was dosed at 8 μM , leading to a decrease in hepatic extraction to 0.41 while propranolol's ER remained high (0.91). This reduction in ER was similar to the effect of quinine: that is, co-dosing of this potent OCT (Oct) inhibitor with GNE1 and propranolol in a cassette resulted in significant reduction in the victims' ER (0.36 and 0.45, respectively). A separate *in vitro* experiment was

Table 3. Summary of experimental results from isolated perfused rat liver experiment.

Isolated Perfused Rat Liver ^a	GNE1 $C_{in} = 0.3 \mu\text{M}$	GNE1 $C_{in} = 8 \mu\text{M}$	GNE1 $C_{in} = 0.3 \mu\text{M}$ with Quinine (10 μM)
GNE1 hepatic ER	0.78	0.41	0.36
^b Propranolol (cassette) ER	>0.95	0.91	0.45
Biliary clearance	0.7 mL/min/kg	0.23 mL/min/kg	0.046 mL/min/kg
Total liver concentration of GNE1	8 μM		
^c Perfusate C_{out}	0.07 μM		
f_u perfusate and f_u in liver (corrected)	0.3/0.01		
$k_{p_{u,u}}$	3.8		

^aSingle pass flow rate = 12 mL/min

^bPropranolol concentration = 2 to 4 μM .

^cPerfusate contained oxygenated 20% bovine red blood cells and 4% bovine serum albumin to maintain liver function throughout the experiment.

C_{in} , concentration of drug entering the liver; C_{out} , concentration of drug exiting the liver; ER, extraction ratio; f_u , the unbound fraction; $K_{p_{u,u}}$, intracellular to extracellular ratio of unbound concentrations.

conducted, and quinine was found to inhibit propranolol metabolism at 1-10 micromolar concentrations (data not shown).

DISCUSSION

In enzyme kinetics, the rate-determining or rate-limiting step is used interchangeably to describe the slowest step in the overall reaction [28]. However, to properly describe the disappearance of a drug from systemic circulation and the elimination of a drug from tissues and whole body, the rate-determining and rate-limiting steps need to be redefined; the former describes the fastest step in the disappearance from systemic circulation after an IV dose [5, 29], and the latter describes the slowest step in elimination from the whole body. Previously, we have shown that GNE1 was rapidly taken up by rat hepatocytes with an uptake rate ($CL_{int, influx}$) comparable to that of atorvastatin in cryo-preserved rat hepatocytes (11.1 vs. 12.6 mL/min/g of liver, respectively) [1]. The rate-determining step in the clearance of atorvastatin is mediated by Oatp uptake in rat, and, therefore, this compound was used as our benchmark reference [5]. OCT1 was identified to be the key transporter for GNE1 for the uptake both *in vitro* (OCT1 transfected cells and quinine as inhibitor) and *in vivo* (Oct KO animals). Because of the commercial availability of Oct KO mice and the sequence homology between mouse and rat Oct1 (95%) [30], the former was selected as the model for us to probe the rate-determining step in clearance. *In vitro*, ABT at 500 μ M completely inhibited both oxidative and *N*-acetylation metabolism in mouse hepatocytes (supplemental data). This is consistent with the literature showing that the pan-P450 inhibitor, ABT, is also a potent inhibitor of *N*-acetyltransferase [31]. Based on this paper by Sun *et al.*, when ABT was dosed orally *in vivo* at 100 mg/kg (2 h predose) with procainamide (IV), the clearance of procainamide was reduced by 45%. Using a similar experimental protocol, however, GNE1 clearance was reduced only by 20.5% in wild-type versus 28.2% in Oct KO mice. By contrast, the blood clearance of GNE1 was reduced by an average of 56% in Oct KO animals. This decrease reflects organ blood flow-limited clearance to about half its value. The plasma concentration of ABT reached 752 μ M at C_{max} with a long elimination half-life [32]. Taken together, these data further confirmed that the rate-determining step in the clearance of GNE1 is cellular uptake rather than metabolism, and this is likely the major source of the IVIV disconnect in clearance.

To ensure accurate measurement of PK parameters, IV infusion experiment to steady state was carried out in addition to bolus administration. However because clearance of GNE1 exceeded hepatic blood flow in rat even after such infusion, additional experiments were conducted to 1) understand hepatic contribution *via* IPL and 2) excreta were collected from both intact and BDC rats to understand the major elimination pathway. It was found that the hepatic ER was concentration-dependent (Table 3), which is consistent with transporter-mediated active uptake kinetics [5]. Propranolol behaved as expected with high hepatic extraction due to metabolism (data not shown). At a higher GNE1 substrate concentration (8 vs. 0.3 μ M), hepatic extraction ratio was reduced by about half (0.41 vs. 0.78, respectively). No significant drug-drug interaction was

observed when propranolol was co-dosed with GNE1. Biliary clearance was low consistently throughout multiple IPL experiments, and it accounted for less than 5% of the total perfusate clearance. Recoveries of GNE1 and its major acetylated metabolite GNE4 were also low in the perfusing outlet, suggesting a significant trapping of GNE1 in the liver compartment (Fig. 3). The unbound tissue/perfusate ratio was significantly greater than one, further confirming that the rate of influx was significantly higher than the rate of elimination either by metabolism or canalicular efflux. This result is also consistent with the intracellular unbound concentration model developed by Pfeifer *et al.* [26] and the classification system described by us [1]. Addition of a potent OCT/Oct1 inhibitor, quinine, also reduced the hepatic ER by about 2-fold, but metabolism of propranolol was also reduced. Therefore, a more selective Oct1 inhibitor will be needed for this type of study in the future. Nevertheless, taken together, this set of data suggests that free plasma concentration (i.e., the free drug hypothesis) is no longer a good reflection of free tissue concentration for GNE1 in rat. The unbound tissue concentration depends on the expression level of OCT/Oct transporters in different organs in human and rat, respectively. Therefore, if transporter-mediated influx into a tissue is higher than the rate of elimination by either metabolism or efflux, tissue accumulation of the test article will occur. Ultimately, both pharmacodynamic and toxicity may dependent more on intracellular tissue concentration than on plasma concentration for molecules of this class.

IPL experiments showed that both metabolism and biliary excretion of GNE1 were slow despite a high hepatic extraction ratio. After collecting excreta from intact rats, we found that majority of the IV dose was recovered as unchanged parent molecule ($77 \pm 36\%$) in feces. This less-than-ideal recovery and high variability are likely due to incomplete collection of feces at the end of experiment because in the second set of experiments, in which the excreta were collected up to 72 hours, both the recovery and variability were improved dramatically (Table 2B and 2C). The amount of GNE1 detected in urine accounted for only 15.6% of the total dose over a 24 hour collection period. However, because renal clearance of GNE1 was about 4-fold higher than the glomerular filtration rate (20 vs. 5 mL/min/kg, respectively), active secretion of GNE1 is likely. It is not clear at this point which efflux transporters are involved in the elimination of GNE1. No effort to further was made characterize the efflux transporter(s) involved because of the slow biliary excretion.

The *N*-acetylated metabolite, GNE4, accounted for an additional 9.5% of the total dose, and no other oxidative metabolites were detected, further confirming that metabolism was only a minor player in the elimination of GNE1. Stability of GNE4 in rat intestinal S9 and feces were also tested and it was stable to hydrolysis (data not shown) suggesting degradation of this metabolite back to GNE1 in the gut is unlikely. Because a majority of the dose was found unchanged in feces and biliary excretion of the parent molecule is slow, the data suggest that intestinal secretion, either *via* slow passive diffusion and/or secretion *via* efflux transporters, is the major elimination pathway and might be the rate-limiting (slowest) step in the "total" elimination of

GENE1 from rat. To confirm this, we conducted a separate BDC study in rats. Indeed the amount of GNE1 detected in bile was also low, which is consistent with earlier *ex vivo* experiments.

While the recovery of GNE1 was not complete even after 72 hours of collection in BDC rats, the amount of unchanged test article detected in feces after diversion of bile flow was 31% (Table 2C), further confirming that intestinal secretion is an important pathway for the elimination of GNE1 and the process is likely slower than hepatic uptake because of slow metabolism and efflux. In fact, despite rapid disappearance of GNE1 in plasma, the amount of GNE1 detected in urine was highest (30%) during the 4–8 hour time period and in feces, the highest amount (18%) was observed during 8–24 hours over a 24 hour collection period. It is not clear at this point why the percentage of GNE1 detected in urine from BDC rats is about 2-fold higher than that in intact rats (30 vs. 15%, respectively), and also why the total amount of GNE1 is significantly lower in BDC rats than in intact rats (consistently lower in both 24 and 72 h collection). This type of inconsistency has also been reported for rifapentine [33]. In this molecule, total radioactivity recovery of dose was about 100% in uncannulated rats with a vast majority of the dose recovered in feces (approximately 3% was recovered in the carcass), but recovery was only 41.1% in cannulated rats, with 41.7% of the radioactivity recovered from the carcass. Invasive surgery may alter the pathway of elimination, and, therefore, data should be interpreted with caution. It is possible that diversion of bile flow in cannulated rats may have impaired intestinal secretion.

Intestinal secretion as one of the major elimination pathways has been reported in the past for drugs such as apixaban, ivermectin, and rifapentine [33-35]. Similar to GNE1, the major elimination pathway in rats for these examples is active secretion rather than metabolism. Oct1 is heavily expressed on the sinusoidal side of rodent intestine and kidney in addition to the liver [30]. Interestingly in human, OCT1 is highly expressed only in liver but less so in kidney and intestine. The extrahepatic expression of Oct1 is the likely explanation for the higher than hepatic blood flow clearance observed for GNE1. On the basis of these data, it is reasonable to conclude that the intestine is one of the key eliminating organs for GNE1. Future work to include intestinal loop models [35] to examine the uptake and secretion of GNE in rat is warranted. Finally, because of extrahepatic Oct1 involvement in the clearance of GNE1 in rodent, significant under-prediction of clearance is expected if only using hepatic uptake data generated *in vitro*.

CONCLUSION

One of the most challenging pharmacokinetic parameters to unequivocally determine in drug discovery is perfusion-limited (high lipoidal passive permeability) and permeability-limited (low lipoidal passive permeability) clearance [2]. Recently, two new classification systems for the prediction of clearance mechanisms in drug discovery have been published [1, 36]: the permeability-based Hepatic Clearance Classification System and the Extended Clearance Classification System. The former describes the rapid transporter-mediated influx of a poorly permeable compound

and accumulation in the liver when elimination is slow (class T1) [1]. The latter predicts that renal clearance should be a major elimination pathway for basic and poorly permeable compounds. Given that both systems were designed to predict the major clearance mechanism(s) in a drug discovery setting, it is interesting to note that GNE1, which is a triprotic base with calculated PKa values of 9.43, 4.82 and 3.10, is poorly permeable in MDCK parent cells, and yet we found that both biliary and renal elimination are low, at about 14 and 16% of the total clearance, respectively. Instead, intestinal secretion (non-biliary) was the major elimination pathway for this class of molecule after IV dose, since a majority of the unchanged GNE1 was found in feces, with slow biliary excretion from both BDC rats and IPL experiments. Therefore, more research in this area is needed before we can accurately predict the major elimination route(s) in different species.

LIST OF ABBREVIATIONS

ABT	=	1-aminobenzotriazole
BDC	=	bile-duct cannulated
ER	=	extraction ratio
IVIV	=	<i>in vitro-in vivo</i> correlation
f_u	=	fraction unbound
K_p	=	liver to perfusate partition coefficient
$K_{p_{u,u}}$	=	unbound liver to unbound perfusate partition coefficient
PAK1	=	p21-activated kinase member 1
Oct1/2	=	organic cation transporter 1/2 or solute carrier family 22 member 1/2 (Slc22a1/2).

CONFLICT OF INTEREST

The authors confirm that this article content has no conflict of interest.

ACKNOWLEDGEMENTS

Declared none.

REFERENCES

- [1] Fan, P.W.; Song, Y.; Berezhkovskiy, L.M.; Cheong, J.; Plise, E.G.; Khojasteh, S.C. Practical permeability-based hepatic clearance classification system (HepCCS) in drug discovery. *Future Med. Chem.*, **2014**, *6*, 1995-2012.
- [2] Rowland, M.; Tozer, T. *Clinical Pharmacokinetics Concepts and Applications*, 3rd Ed.; Lippincott Williams & Wilkins: Philadelphia, **1995**.
- [3] Lipinski, C.A.; Lombardo, F.; Dominy, B.W.; Feeney, P.J. Experimental and computational approaches to estimate solubility and permeability in drug discovery and development settings. *Adv. Drug Deliv. Rev.*, **2001**, *46*, 3-26.
- [4] Houston, J.B. *Transporters and Cytochrome P450 Interplay in Defining Hepatic Drug Clearance*. 4th European Cyprotex Drug Discovery Workshop. London, UK, **2010**.
- [5] Watanabe, T.; Kusuhara, H.; Maeda, K.; Kanamaru, H.; Saito, Y.; Hu, Z.; Sugiyama, Y. Investigation of the rate-determining process in the hepatic elimination of HMG-CoA reductase inhibitors in rats and humans. *Drug Metab. Dispos.*, **2010**, *38*, 215-222.

- [6] Soars, M.G.; Grime, K.; Sproston, J.L.; Webborn, P.J.; Riley, R.J. Use of hepatocytes to assess the contribution of hepatic uptake to clearance *in vivo*. *Drug Metab. Dispos.*, **2007**, *35*, 859-865.
- [7] Hallifax, D.; Houston, J.B. Saturable uptake of lipophilic amine drugs into isolated hepatocytes: mechanisms and consequences for quantitative clearance prediction. *Drug Metab. Dispos.*, **2007**, *35*, 1325-1332.
- [8] Umehara, K.; Camenisch, G. Novel *in vitro-in vivo* extrapolation (IVIVE) method to predict hepatic organ clearance in rat. *Pharm. Res.*, **2012**, *29*, 603-617.
- [9] Swift, B.; Pfeifer, N.D.; Brouwer, K.L. Sandwich-cultured hepatocytes: an *in vitro* model to evaluate hepatobiliary transporter-based drug interactions and hepatotoxicity. *Drug Metab. Rev.*, **2010**, *42*, 446-471.
- [10] Zhao, Z.S.; Manser, E. PAK family kinases: Physiological roles and regulation. *Cell Logist.*, **2012**, *2*, 59-68.
- [11] Ong, C.C.; Jubb, A.M.; Haverty, P.M.; Zhou, W.; Tran, V.; Truong, T.; Turley, H.; O'Brien, T.; Vucic, D.; Harris, A.L.; Belvin, M.; Friedman, L.S.; Blackwood, E.M.; Koeppen, H.; Hoeflich, K.P. Targeting p21-activated kinase 1 (PAK1) to induce apoptosis of tumor cells. *Proc. Natl. Acad. Sci. USA*, **2011**, *108*, 7177-7182.
- [12] Ong, C.C.; Jubb, A.M.; Jakubiak, D.; Zhou, W.; Rudolph, J.; Haverty, P.M.; Kowanetz, M.; Yan, Y.; Tremayne, J.; Lisle, R.; Harris, A.L.; Friedman, L.S.; Belvin, M.; Middleton, M.R.; Blackwood, E.M.; Koeppen, H.; Hoeflich, K.P. P21-activated kinase 1 (PAK1) as a therapeutic target in BRAF wild-type melanoma. *J. Natl. Cancer Inst.*, **2013**, *105*, 606-607.
- [13] Zhou, W.; Jubb, A.M.; Lyle, K.; Xiao, Q.; Ong, C.C.; Desai, R.; Fu, L.; Gnad, F.; Song, Q.; Haverty, P.M.; Aust, D.; Grutzmann, R.; Romero, M.; Totpal, K.; Neve, R.M.; Yan, Y.; Forrest, W.F.; Wang, Y.; Raja, R.; Pilarsky, C.; De Jesus-Acosta, A.; Belvin, M.; Friedman, L.S.; Merchant, M.; Jaffee, E.M.; Zheng, L.; Koeppen, H.; Hoeflich, K.P. PAK1 mediates pancreatic cancer cell migration and resistance to MET inhibition. *J. Pathol.*, **2014**, *234*, 502-513.
- [14] Crawford, J.J.; Hoeflich, K.P.; Rudolph, J. p21-Activated kinase inhibitors: a patent review. *Expert Opin. Ther. Pat.*, **2012**, *22*, 293-310.
- [15] Rudolph, J.; Crawford, J.J.; Hoeflich, K.P.; Chernoff, J. p21-activated kinase inhibitors. *Enzymes*, **2013**, *34* (Pt. B), 157-180.
- [16] Rudolph, J.; Crawford, J.J.; Hoeflich, K.P.; Wang, W. Inhibitors of p21-Activated Kinases (PAKs). *J. Med. Chem.*, **2015**, *58*, 111-129.
- [17] Crawford, J.J.; Lee, W.; Aliagas, I.; Mathieu, S.; Hoeflich, K.P.; Zhou, W.; Wang, W.; Rouge, L.; Murray, L.; La H.; Fan P.W.; Liu N.; Cheong J.; Heise C.E.; Ramaswamy S.; Mintzer R.; Liu Y.; Chao Q.; Rudolph J. Structure-guided design of group I selective p21-activated kinase inhibitors. *J. Med. Chem.*, **2015**, *58*, 5121-5136.
- [18] Barker, D.F.; Walraven, J.M.; Ristagno, E.H.; Doll, M.A.; States, J.C.; Hein, D.W. Quantitative tissue and gene-specific differences and developmental changes in Nat1, Nat2, and Nat3 mRNA expression in the rat. *Drug Metab. Dispos.*, **2008**, *36*, 2445-2451.
- [19] Loureiro, A.I.; Fernandes-Lopes, C.; Bonifacio, M.J.; Wright, L.C.; Soares-Da-Silva, P. N-acetylation of etamicastat, a reversible dopamine-beta-hydroxylase inhibitor. *Drug Metab. Dispos.*, **2013**, *41*, 2081-2086.
- [20] Jia, L.; Liu, X. The conduct of drug metabolism studies considered good practice (II): *in vitro* experiments. *Curr. Drug Metab.*, **2007**, *8*, 822-829.
- [21] Jones, H.M.; Houston, J.B. Substrate depletion approach for determining *in vitro* metabolic clearance: time dependencies in hepatocyte and microsomal incubations. *Drug Metab. Dispos.*, **2004**, *32*, 973-982.
- [22] Zhang, D.; Luo, G.; Ding, X.; Lu, C. Preclinical experimental models of drug metabolism and disposition in drug discovery and development. *Acta Pharm. Sinica B*, **2012**, *2*, 549-561.
- [23] Mehvar, R.; Reynolds, J. Input rate-dependent stereoselective pharmacokinetics. Experimental evidence in verapamil-infused isolated rat livers. *Drug Metab. Dispos.*, **1995**, *23*, 637-641.
- [24] Khojasteh, S.C.; Yue, Q.; Ma, S.; Castanedo, G.; Chen, J.Z.; Lyssikatos, J.; Mulder, T.; Takahashi, R.; Ly, J.; Messick, K.; Jia, W.; Liu, L.; Hop, C.E.; Wong, H. Investigations into the mechanisms of pyridine ring cleavage in vismodegib. *Drug Metab. Dispos.*, **2014**, *42*, 343-351.
- [25] Kalvass, J.C.; Maurer, T.S.; Pollack, G.M. Use of plasma and brain unbound fractions to assess the extent of brain distribution of 34 drugs: comparison of unbound concentration ratios to *in vivo* p-glycoprotein efflux ratios. *Drug Metab. Dispos.*, **2007**, *35*, 660-666.
- [26] Pfeifer, N.D.; Harris, K.B.; Yan, G.Z.; Brouwer, K.L. Determination of intracellular unbound concentrations and subcellular localization of drugs in rat sandwich-cultured hepatocytes compared with liver tissue. *Drug Metab. Dispos.*, **2013**, *41*, 1949-1956.
- [27] Lau, Y.Y.; Okochi, H.; Huang, Y.; Benet, L.Z. Pharmacokinetics of atorvastatin and its hydroxy metabolites in rats and the effects of concomitant rifampicin single doses: relevance of first-pass effect from hepatic uptake transporters, and intestinal and hepatic metabolism. *Drug Metab. Dispos.*, **2006**, *34*, 1175-1181.
- [28] Steinfeld, J.I.; Francisco, J.S.; Hase, W.L. *Chemical kinetics and Dynamics*, 2nd Ed.; Prentice Hall: Upper Saddle River, NJ, **1999**.
- [29] Parker, A.J.; Houston, J.B. Rate-limiting steps in hepatic drug clearance: comparison of hepatocellular uptake and metabolism with microsomal metabolism of saquinavir, nelfinavir, and ritonavir. *Drug Metab. Dispos.*, **2008**, *36*, 1375-1384.
- [30] Koepsell, H.; Lips, K.; Volk, C. Polyspecific organic cation transporters: structure, function, physiological roles, and biopharmaceutical implications. *Pharm. Res.*, **2007**, *24*, 1227-1251.
- [31] Sun, Q.; Harper, T.W.; Dierks, E.A.; Zhang, L.; Chang, S.; Rodrigues, A.D.; Marathe, P. 1-Aminobenzotriazole, a known cytochrome P450 inhibitor, is a substrate and inhibitor of N-acetyltransferase. *Drug Metab. Dispos.*, **2011**, *39*, 1674-1679.
- [32] Balani, S.K.; Li, P.; Nguyen, J.; Cardoza, K.; Zeng, H.; Mu, D.X.; Wu, J.T.; Gan, L.S.; Lee, F.W. Effective dosing regimen of 1-aminobenzotriazole for inhibition of antipyrine clearance in guinea pigs and mice using serial sampling. *Drug Metab. Dispos.*, **2004**, *32*, 1092-1095.
- [33] Emary, W.B.; Toren, P.C.; Mathews, B.; Huh, K. Disposition and metabolism of rifapentine, a rifamycin antibiotic, in mice, rats, and monkeys. *Drug Metab. Dispos.*, **1998**, *26*, 725-731.
- [34] Zhang, D.; Frost, C.E.; He, K.; Rodrigues, A.D.; Wang, X.; Wang, L.; Goosen, T.C.; Humphreys, W.G. Investigating the enteroenteric recirculation of apixaban, a factor Xa inhibitor: administration of activated charcoal to bile duct-cannulated rats and dogs receiving an intravenous dose and use of drug transporter knockout rats. *Drug Metab. Dispos.*, **2013**, *41*, 906-915.
- [35] Laffont, C.M.; Toutain, P.L.; Alviner, M.; Bousquet-Melou, A. Intestinal secretion is a major route for parent ivermectin elimination in the rat. *Drug Metab. Dispos.*, **2002**, *30*, 626-630.
- [36] Varma, M.V.; Steyn, S.J.; Allerton, C.; El-Kattan, A.F. Predicting clearance mechanism in drug discovery: Extended clearance classification system (ECCS). *Pharm. Res.*, **2015**, *32*, 3785-3802.